DOI: 10.1002/ejic.200700304

Cleavage of CO by Mo[N(R)Ar]$_3$ Complexes

Gemma Christian,[a] Robert Stranger,*[a] Brian F. Yates,[b] and Christopher C. Cummins[c]

Keywords: C–O activation / Molybdenum / Three-coordinate complexes / Density functional calculations / Bond cleavage

The reaction of MoL_3 [L = NH_2 and N(*t*Bu)Ar] with CO was explored using DFT in order to rationalize why CO cleavage is not observed experimentally for this system in contrast to the corresponding N_2 reaction which results in spontaneous cleavage of the N–N bond. The binding of CO to MoL_3 was found to be both kinetically and thermodynamically favored over the binding of N_2, with the formation of the encounter complex, L_3Mo–CO, calculated to be without barrier and exothermic. While the overall reaction to form the C–MoL_3 and O–MoL_3 products was calculated to be energetically favorable, both the encounter complex and intermediate dimer, L_3Mo–CO–MoL_3, were found to be lower in energy than the products, with the final C–O cleavage step calculated to be endothermic by 169 kJ mol^{-1} and 163 kJ mol^{-1} for L = NH_2 and N(*t*Bu)Ar, respectively. The unfavorable CO cleavage step can be attributed to the fact that Mo does not possess the optimum d-electron configuration to sufficiently stabilise the carbide and oxide products relative to the CO-bridged intermediate dimer.

Introduction

One of the most significant discoveries in dinitrogen chemistry is the cleavage of N_2 by Mo[N(*t*Bu)Ar]$_3$ under mild conditions.[1,2] N_2 reacts with Mo[N(*t*Bu)Ar]$_3$ to form the intermediate dimer, [Ar(*t*Bu)N]$_3$Mo–N_2–Mo[N(*t*Bu)Ar]$_3$, with N_2 bridging the metal centers end-on, followed by N–N bond cleavage to form the nitride product N–Mo[N(*t*Bu)Ar]$_3$.[3–5] The reaction proceeds under mild conditions (1 atm of pressure and between –33 and 25 °C) compared with the extreme conditions of 200 atm and 500 °C required in the industrial Haber–Bosch process for nitrogen fixation. In addition to N_2 cleavage, Mo[N(*t*Bu)Ar]$_3$ is also known experimentally to cleave the stronger N–N bond in N_2O to form the nitride, N–Mo[N(*t*Bu)Ar]$_3$, and nitrosyl, [Ar(*t*Bu)N]$_3$Mo–NO, products.[6,7]

Following the success of N_2 and N_2O cleavage by Mo[N(R)Ar]$_3$ complexes under mild conditions, attention was turned to other small multiply bonded molecules such as CO and CN^-. Although CO and CN^- are isoelectronic with N_2, and therefore in principle Mo[N(R)Ar]$_3$ complexes are able to provide the necessary number of electrons to reductively cleave these small molecules, to date neither C–O or C–N bond cleavage has been observed.[8–10] The carbide complex [C–Mo[N(*t*Bu)Ar]$_3$]$^-$ has been synthesized from the encounter complex, [Ar(*t*Bu)N]$_3$Mo–CO, the latter easily formed by the reaction of Mo[N(*t*Bu)Ar]$_3$ with CO.[8] However, despite the ready formation of the encounter complex, neither the intermediate dimer or C–O cleavage is observed and instead, the O atom in the [Ar(*t*Bu)N]$_3$Mo–CO complex is removed through conversion to the related methylidene complex, [HC–Mo[N(*t*Bu)Ar]$_3$], which is then deprotonated to form [C–Mo[N(*t*Bu)Ar]$_3$]$^-$.[8,9]

The resistance of CO to cleavage by Mo[N(R)Ar]$_3$ complexes may well be a consequence of the fact that the bond dissociation energy for CO is approximately 100 kJ mol^{-1} greater than that for N_2. However, an alternative view is that the metals used to form the intermediate dimer, in this case only Mo, are not tuned to optimise the thermodynamics of the cleavage reaction. This aspect is particularly pertinent since a recent theoretical study[11] has shown that CO cleavage is predicted to be spontaneous under mild conditions when two different three-coordinate complexes Re[N(R)Ar]$_3$ and Ta[N(R)Ar]$_3$ are used. In this reaction, an intermediate dimer is formed with Re[N(R)Ar]$_3$ and Ta[N(R)Ar]$_3$ binding to the C and O atoms, respectively, and cleavage of CO proceeds without barrier.

The reaction steps of [Ar(*t*Bu)N]$_3$Mo with CO are shown in Scheme 1, assuming the cleavage of CO proceeds by a mechanism analogous to the N_2 cleavage reaction. The first step involves the binding of CO to form the encounter complex, [Ar(*t*Bu)N]$_3$Mo–CO, followed by binding of a second Mo[N(*t*Bu)Ar]$_3$ unit to form [Ar(*t*Bu)N]$_3$Mo–CO–Mo[N(*t*Bu)Ar]$_3$, and finally C–O bond cleavage to give the products C–Mo[N(*t*Bu)Ar]$_3$ and O–Mo[N(*t*Bu)Ar]$_3$.

[a] Department of Chemistry, Faculty of Science,
Australian National University, Canberra, ACT 0200, Australia
Fax: +61-2-6125-0760
E-mail: rob.stranger@anu.edu.au
[b] School of Chemistry, University of Tasmania,
Private Bag 75, Hobart, TAS 7001, Australia
[c] Department of Chemistry, Massachusetts Institute of Technology,
Cambridge, MA 02139, USA

Supporting information for this article is available on the WWW under http://www.eurjic.org or from the author.

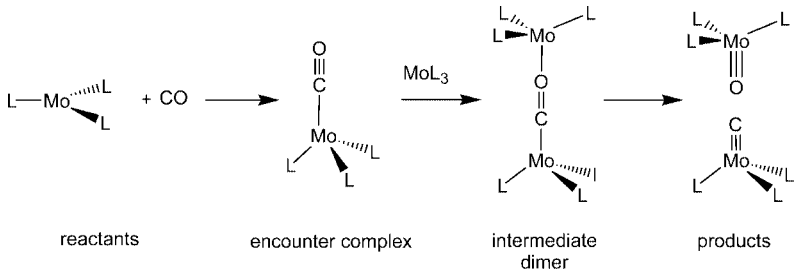

Scheme 1. The reaction of CO with MoL_3, L = NH_2 or N(*t*Bu)Ar.

In this study, the reaction mechanism shown in Scheme 1 is explored using density functional theory (DFT) for both the model, L = NH_2, and experimental, L = N(*t*Bu)Ar, systems in order to rationalise the experimental results. Earlier work on the analogous N_2 cleavage reaction by us and other groups[5,12–14] has shown that DFT methods give results in good agreement with experiment.

Results and Discussion

1.1 Calculated Structures

For the model system (L = NH_2), calculations were carried out on the encounter complex, $[H_2N]_3Mo–CO$ and intermediate dimer, $[H_2N]_3Mo–CO–Mo[NH_2]_3$. The energies and structures of the remaining species, namely the reactant, $[H_2N]_3Mo$, and products, $[H_2N]_3Mo–C$ and $[H_2N]_3Mo–O$, have been reported in earlier studies.[13,15] In the case of the experimental system [L = N(*t*Bu)Ar], QM/MM calculations were carried out for the reactant, encounter complex, intermediate dimer and products. The optimized model and QM/MM structures are shown in Figure 1 and selected structural data from these calculations are shown in Table 1.

For the model system, the reaction of $[H_2N]_3Mo$ with CO gives rise to two possible encounter complexes, $[H_2N]_3Mo–CO$ [structure (c)] and $[H_2N]_3Mo–OC$. Both complexes have doublet ground states with approximately C_s symmetry with one amide ligand rotated by 90° around the metal–ligand axis. The Mo–C–O angle of 177° indicates that the Mo–CO fragment is slightly distorted from linear geometry. Similar ligand rotation has been found for the analogous dinitrogen complex $[H_2N]_3Mo–N_2$.[13,16] The model and QM/MM structures of the CO encounter complex [structures (c) and (d)] have very similar core structures and bond lengths. Because the formation of the O-bound encounter complex was calculated to be endothermic, it is not considered further.

For the model system, the optimized C_s structure of the intermediate dimer [structure (e)] has a bent Mo–C–O–Mo core with a C–O–Mo bond angle of 126° in the triplet spin state. In the QM/MM system [structure (f)], bending of the core is also observed but the larger size of the N(*t*Bu)Ar ligands restricts the C–O–Mo bond angle to 163°. Analogous to the N_2-bridged intermediate dimer,[13,16] ligand rotation around the metal–N(amide) axis is also observed for the CO-bridged intermediate dimer. However, while ligand rotation is observed at only one metal center for the model

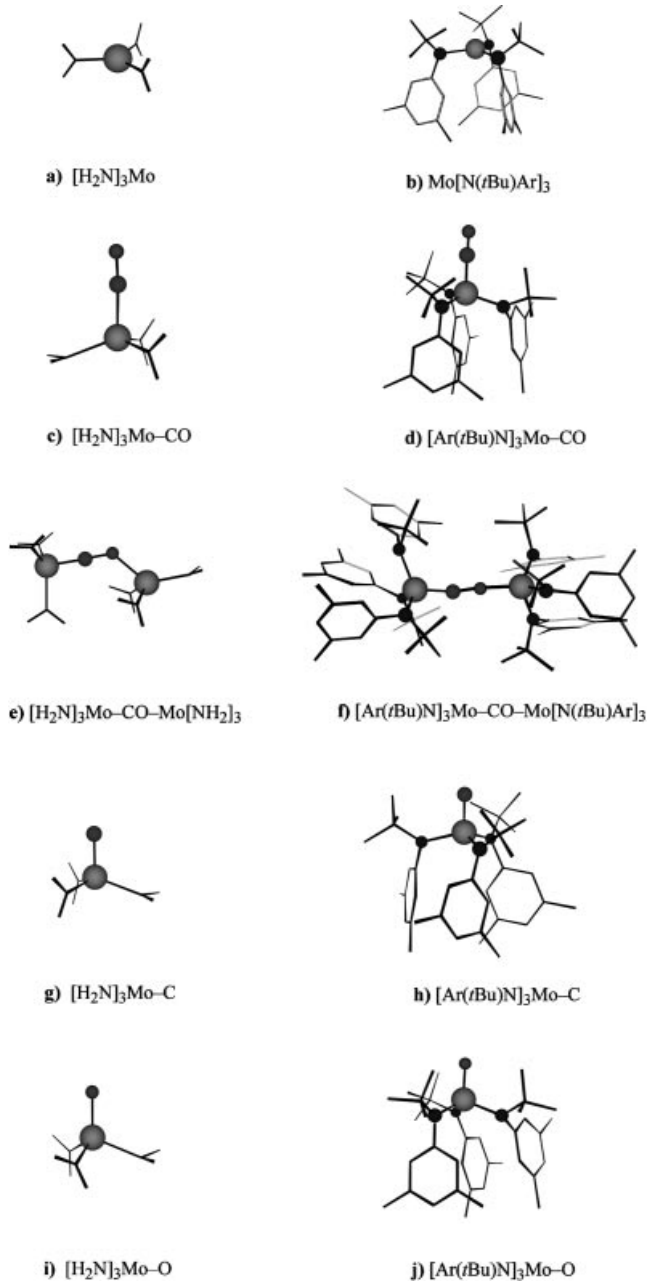

Figure 1. Optimized model and QM/MM structures.

Table 1. Selected geometric parameters for encounter complex, intermediate dimer and products.

Complex	L	Spin	Bond lengths [Å]			Bond angles [°]	
			CO	Mo–C/Mo–O	Mo–N_{amide}	C–Mo–N/O–Mo–N	Mo–C–O/Mo–O–C
L_3Mo	NH_2	3/2			1.982		
	N(*t*Bu)Ar				2.004		
L_3Mo–CO	NH_2	1/2	1.184	1.921	1.969	103	177
	N(*t*Bu)Ar		1.184	1.906	1.989	103	177
L_3Mo–CO–MoL_3	NH_2[a]	0	1.294	1.774/1.960	1.960	101/115	178/134
	N(*t*Bu)Ar		1.276	1.823/1.957	1.987	107/113	168/175
	NH_2[a]	1	1.278	1.789/2.048	1.974	100/104	178/126
	N(*t*Bu)Ar		1.272	1.815/2.019	1.999	105/110	177/163
L_3Mo–C	NH_2	1/2		1.760	1.982	105	
	N(*t*Bu)Ar			1.737	1.994	105	
L_3Mo–O	NH_2	1/2		1.722	1.975	113	
	N(*t*Bu)Ar			1.717	1.996	111	

[a] Data has been included for the model intermediate dimer $[H_2N]_3Mo$–CO–$Mo[NH_2]_3$ even though the optimized structure is not a true minimum.

system, it occurs at both metal centers for the QM/MM system. This difference between the model and QM/MM structures is a consequence of the fact that rotation of the bulky N(tBu)Ar ligands has been shown to reduce steric crowding.[16]

The $[Ar(tBu)N]_3Mo$–C product [structure (h)] has approximately trigonal symmetry, unlike $[H_2N]_3Mo$–C, $[H_2N]_3$-Mo–O and $[Ar(tBu)N]_3Mo$–O [structures (g), (i) and (j)] which all show rotation of one or more of the amide ligands. However, the QM/MM structure for $[Ar(tBu)N]_3$-Mo–C with one ligand rotated lies only 11 kJ mol^{-1} higher in energy. In general, the metal–amide distances are greater for L = N(*t*Bu)Ar than L = NH_2, consistent with the increased steric crowding for the former ligand. The C–O bond lengths of 1.278 and 1.276 Å in the lowest energy model and QM/MM intermediate dimer structures, respectively, indicate moderate activation compared to free CO (cf. 1.128 Å).

1.2 Overall Reaction Profile

The relative energies of species along the reaction pathway for the cleavage of CO by MoL_3 are summarized in Table 2 for both the model and QM/MM systems. The corresponding energies of species in the analogous N_2 cleavage reaction are also included for comparison. Overall, the CO cleavage reaction is exothermic for the model and experimental systems but the encounter complex and intermediate dimer are lower in energy than the products in both systems. Cleavage of the C–O bond to form L_3Mo–C and L_3Mo–O is highly unfavorable, and is calculated to be endothermic by 169 and 163 kJ mol^{-1} for the model and experimental systems, respectively. In general, when L = N(*t*Bu)Ar, the reaction of MoL_3 with CO is less exothermic and the species along the reaction pathway are less stable relative to reactants than when L = NH_2. This is consistent with the results for the N_2 cleavage reaction where a similar decrease in exothermicity was found when L = N(*t*Bu)Ar due to increased steric crowding.

Table 2. Calculated energies of the encounter complex, dimer and products relative to reactants for the reaction of CO and N_2 with MoL_3 for L = NH_2 and N(*t*Bu)Ar.[13]

Reaction	L	Encounter complex	Dimer	Product
CO	NH_2	–152	–248	–79
	N(*t*Bu)Ar	–142	–222	–59
N_2	NH_2	–71	–241	–335
	N(*t*Bu)Ar	–43	–238	–293

From the data in Table 2, the intermediate dimer is calculated to be the lowest energy species on the reaction pathway, and is 96 and 80 kJ mol^{-1} lower in energy than the encounter complex for L = NH_2 and L = N(*t*Bu)Ar, respectively. However, under the reported experimental conditions, the intermediate dimer is not isolated, and instead the reaction is observed to cease with the formation of the encounter complex $[Ar(tBu)N]_3Mo$–CO.[8,9] Although formation of the dimer is entropically unfavorable, ΔS is calculated to be 218 J mol^{-1}·T^{-1} which is not enough to offset ΔH, even at room temperature.

1.3 Formation of the Encounter Complex and Intermediate Dimer

Because the calculations indicate that the intermediate dimer, L_3Mo–CO–MoL_3, should be thermodynamically stable, then it is pertinent to examine the kinetic barriers that may prevent its formation. Accordingly, the formation of both the L_3Mo–CO encounter complex and intermediate dimer, L_3Mo–CO–MoL_3, for L = NH_2 and N(*t*Bu)Ar, were investigated via linear transits, the results of which are shown in Figure 2.

The formation of the encounter complex, L_3Mo–CO, begins on the spin quartet surface but the spin doublet crosses below the quartet surface to become the minimum at an Mo–C distance of around 1.9 Å. There is no barrier to formation in either spin state for the model or QM/MM systems and the reaction is exothermic by 152 and 142 kJ mol^{-1} for L = NH_2 and N(*t*Bu)Ar, respectively. To put these re-

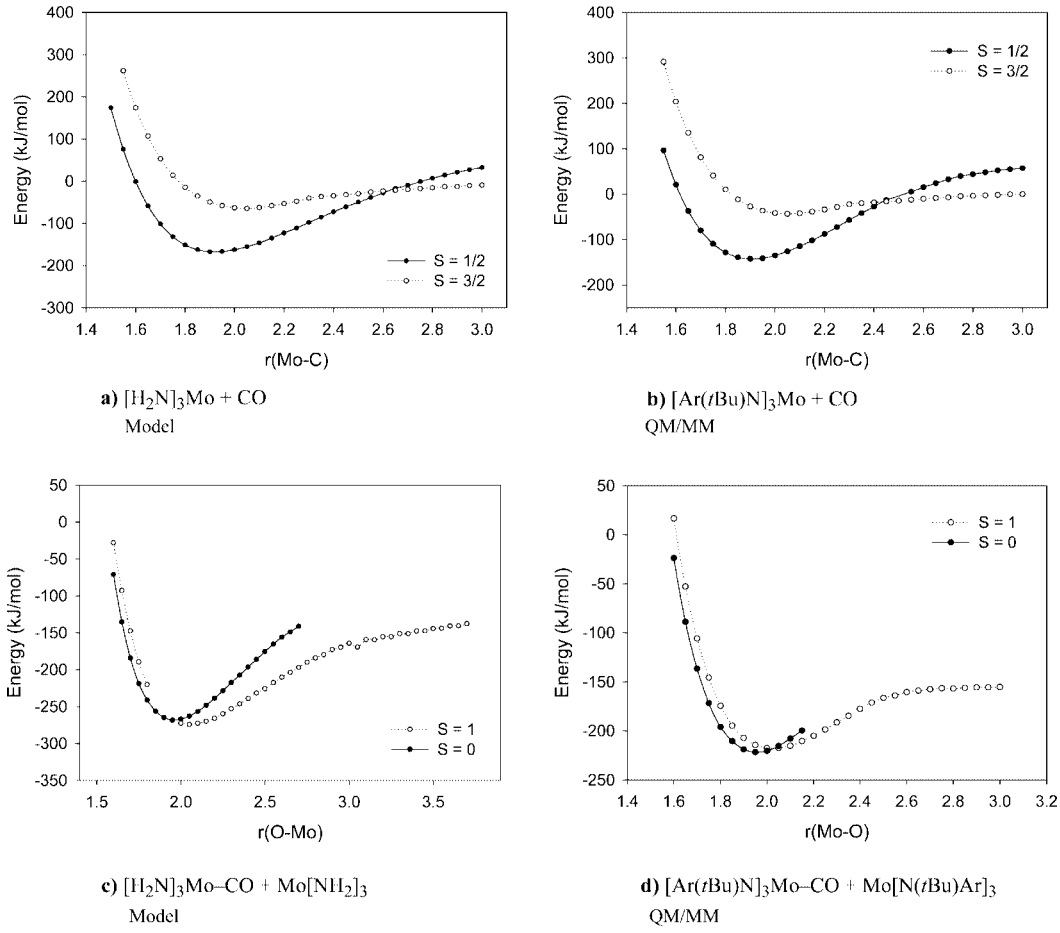

Figure 2. Linear transit results for the formation of (a) $[H_2N]_3Mo–CO$, (b) $[Ar(tBu)N]_3Mo–CO$, (c) $[H_2N]_3Mo–CO–Mo[NH_2]_3$ and (d) $[Ar(tBu)N]_3Mo–CO–Mo[N(tBu)Ar]_3$.

sults in context, the formation of the analogous N_2 encounter complex, $[Ar(tBu)N]_3Mo–N_2$, is exothermic by only 43 kJ mol^{-1} and in addition, has a barrier of approximately 18 kJ mol^{-1}. The uptake of CO by $Mo[N(tBu)Ar]_3$ is therefore both kinetically and thermodynamically much more favorable than the uptake of N_2, consistent with experimental observations in that, while $[Ar(R)N]_3Mo–CO$ has been isolated, $[Ar(R)N]_3Mo–N_2$ has not been observed.[4,17]

Dimer formation for both $[H_2N]_3Mo–CO$ and $[Ar(tBu)N]_3Mo–CO$ through binding of a second MoL_3 complex end-on to O, occurs initially on the spin triplet surface. For L = N(*t*Bu)Ar, the spin singlet state crosses below the triplet when the Mo–O distance is approximately 2.0 Å with the minimum lying at approximately 1.9 Å. For the model system, the spin singlet surface also crosses the triplet around 1.9 Å, but lies higher in energy at the minimum distance of approximately 2.0 Å. As is apparent from Figure 2, there is no barrier to dimer formation for either the model or experimental system.

It is possible that the absence of dimer formation experimentally may be linked to the reaction conditions used. There are two differences in the reported reactions of $Mo[N(tBu)Ar]_3$ with N_2 and CO. Firstly, the solvent used in the CO reaction was tetrahydrofuran (THF) whereas non-polar solvents were used in the reaction with N_2. Secondly, CO, which is bound more easily than N_2, was in excess.

Solvent effects on the reaction energetics were investigated by performing calculations on the model system which allowed binding of THF directly to the reactant, $Mo[NH_2]_3$, encounter complex, $OC–Mo[NH_2]_3$, and the intermediate dimer, $[H_2N]_3Mo–CO–Mo[NH_2]_3$. In the case of the encounter complex, binding of THF to either the Mo or CO was explored. The results are summarized in Table 3.

Table 3. Calculated energies for the binding of THF to $Mo[NH_2]_3$, $[H_2N]_3Mo–CO$ and $[H_2N]_3Mo–CO–Mo[NH_2]_3$.

	ΔE [kJ mol^{-1}]
$[H_2N]_3Mo–THF$	–2
$[H_2N]_3Mo–CO–THF$	ca. 4
THF–$[H_2N]_3Mo–CO$ (*trans*)	–37
$[THF][H_2N]_3Mo–CO–Mo[NH_2]_3$	–13
$[H_2N]_3Mo–CO–Mo[NH_2]_3[THF]$	–38
$[THF][H_2N]_3Mo–CO–Mo[NH_2]_3[THF]$	–59

Binding of THF to the reactant or directly to CO in the encounter complex is predicted to be weak, but binding of THF to Mo (*trans* to CO) in the encounter complex is exothermic by 37 kJ mol^{-1}. Binding of THF to the intermediate dimer is also favorable, particularly when THF is bound at both ends. Although binding of solvent molecules is ex-

pected to be weaker for the experimental system due to ligand crowding, based on these results, the intermediate dimer should be even more stable relative to reactants and encounter complex in the presence of THF. In addition to calculations involving the explicit binding of THF, the effect of the bulk properties of the solvent on the reaction pathway was also studied using the COSMO model. However, the relative energies changed by at most 10 kJ mol^{-1} compared to the unsolvated calculations, and the formation of the dimer is still calculated to be exothermic.

Because the above calculations indicate that solvent effects do not favor formation of the encounter complex over the intermediate dimer, the other main difference in the reaction conditions, namely the presence of excess CO, must be significant. For the N_2 cleavage reaction, binding of N_2 to form the intermediate dimer is known to be slow experimentally,[4] and therefore there is an excess of Mo[N(*t*Bu)Ar]$_3$ available to react with the encounter complex to form the intermediate dimer. Binding of CO to form the encounter complex, [Ar(*t*Bu)N]$_3$Mo–CO, however, is fast and calculated to be more exothermic than the formation of the intermediate dimer. When CO is in excess, the rapid uptake of CO by Mo[N(*t*Bu)Ar]$_3$ will leave little remaining Mo[N(*t*Bu)Ar]$_3$ for dimer formation. However, under different reaction conditions, namely controlling the CO concentration so that it is never in excess, the formation of the [Ar(*t*Bu)N]$_3$Mo–CO–Mo[N(*t*Bu)Ar]$_3$ dimer may be possible.

Conclusions

Calculations were carried out on the reaction of MoL_3 with CO for the model (L = NH_2) and experimental [L = N(*t*Bu)Ar] ligand systems. On the basis of these calculations, the formation of the encounter complex and intermediate dimer are predicted to be thermodynamically favorable and without barrier. Despite the overall cleavage reaction being exothermic, both the encounter complex and intermediate dimer are predicted to be more stable than the O–MoL_3 and C–MoL_3 products and therefore the final C–O cleavage step is unfavorable, being endothermic by 169 and 163 kJ mol^{-1} for the model and experimental systems, respectively. The endothermic CO cleavage step can be rationalized on the basis of the electronic properties of the metal. An earlier study examining M–L bond energies in model [NH_2]$_3$M–L (L = N, C, O) complexes showed that the strongest M–O, M–N and M–C bonds occurred for d^2, d^3 and d^4 metal configurations, respectively.[15] Therefore, in the L_3Mo + CO system, Mo^{III} does not possess the optimum d-electron configuration to sufficiently stabilise the carbide and oxide products relative to the intermediate dimer.

The intermediate dimer, L_3Mo–CO–MoL_3, is calculated to be the lowest energy species along the reaction pathway, and from both a thermodynamic and kinetic perspective, the calculations indicate that its formation is more favorable than the analogous N_2-bound dimer which is observed experimentally in the reaction of Mo[N(*t*Bu)Ar]$_3$ with dinitrogen. Thus, the absence of the CO-bridged intermediate dimer experimentally is attributed to the different reaction conditions employed compared to its N_2 counterpart, namely the use of a polar solvent and the presence of excess CO. Since calculations which investigated solvent effects were shown to favor formation of the CO-bridged intermediate dimer, it is concluded that this species is not observed experimentally due to the presence of excess CO and the ability of Mo[N(*t*Bu)Ar]$_3$ to rapidly bind CO. This conclusion is also consistent with the observation that, while [Ar(*t*Bu)]$_3$Mo–CO has been isolated, [Ar(*t*Bu)]$_3$Mo–N_2 has not been observed experimentally.

Computational Section

The calculations carried out in this work were performed with the Amsterdam Density Functional (ADF)[18–20] program running on either Linux-based Pentium IV computers or the Australian National University Supercomputing Facility. All calculations used the local density approximation (LDA) to the exchange potential, the correlation potential of Vosko, Wilk and Nusair (VWN),[21] the Becke[22] and Perdew[23] corrections for non-local exchange and correlation, and the numerical integration scheme of te Velde and co-workers.[24] Geometry optimizations were performed using the gradient algorithm of Versluis and Ziegler.[25] All electron, triple-ζ Slater-type orbital basis sets (TZP) with polarization functions were used for all atoms. Relativistic effects were incorporated using the zero-order relativistic approximation (ZORA)[26–28] functionality in ADF. Frequency calculations were used to confirm that the optimized model structures of lowest energy were true minima and were computed by numerical differentiation of energy gradients in slightly displaced geometries.[29,30] Solvent-corrected calculations were carried out using the COSMO method[31] to accommodate the bulk effects of the tetrahydrofuran solvent used in the experimental work. For these calculations the solvent dielectric constant was set at 7.58 and the radius (rigid sphere) at 3.18 Å. All calculations were carried out in a spin-unrestricted manner. Optimized structures for the model system were corrected for zero-point vibrational energy. The convergence criteria for geometry optimizations were 10^{-3} Hartrees for energy and 10^{-2} Hartrees/Ångstrom for gradient. SCF convergence was set at 10^{-6}. The integration parameter, accint, was set to 4.0 for geometry optimizations and to 6.0 for frequency calculations. For the experimental M[N(R)Ar]$_3$ system, the QM/MM[32] method implemented in ADF was used. For these calculations, the system under study was partitioned into two regions one of which was treated with DFT and the other with force field methods. The electronically important parts of the molecule were included in the QM region. Accordingly, N_2, CO, the N donors from the amide ligands, and Mo were treated with DFT while the *t*Bu and 3,5-$C_6H_3Me_2$ substituents were treated with molecular mechanics using the Sybyl[33] force field available in ADF. UFF van der Waals parameters[34] were used for Mo and all other parameters involving the metal atoms were set to zero. The bonds that cross the QM/MM partition, known as link bonds, were "capped" by H for the QM region. The ratio of the link bond to the length of the capping bond was kept constant throughout the calculations corresponding to the link bond parameters being fixed at values of $\alpha_{[N–C(R)]}$ = 1.489 and $\alpha_{[N–C(Ar)]}$ = 1.412. All QM/MM calculations on the experimental systems were undertaken in C_1 symmetry.

Supporting Information (see footnote on the first page of this article): Calculated structures and energies for L_3Mo, L_3Mo–CO, L_3Mo–CO–MoL_3, L_3Mo–C and L_3Mo–O for L = NH_2 and N(*t*Bu)Ar. Calculated structures and energies with THF bound to L_3Mo, L_3Mo–CO, L_3Mo–CO–MoL_3, L_3Mo–C and L_3Mo–O for L = NH_2 are also included.

Acknowledgments

The authors gratefully acknowledge the Australian Research Council for financial support in the form of an Australian Postgraduate Award for G. C. and a Discovery Project Grant for R. S. and B. F. Y. The National Science Foundation of the USA is acknowledged for funding support (CHE-0316823) to C. C. C. The Australian National University is also acknowledged for access to the APAC (Australian Partnership for Advanced Computing) supercomputing facilities.

[1] C. C. Cummins, *Chem. Commun.* **1998**, 1777–1786.
[2] S. Gambarotta, J. Scott, *Angew. Chem. Int. Ed.* **2004**, *43*, 5298–5308.
[3] C. E. Laplaza, C. C. Cummins, *Science* **1995**, *268*, 861–863.
[4] C. E. Laplaza, M. J. A. Johnson, J. C. Peters, A. L. Odom, E. Kim, C. C. Cummins, G. N. George, I. J. Pickering, *J. Am. Chem. Soc.* **1996**, *118*, 8623–8638.
[5] Q. Cui, D. G. Musaev, M. Svensson, S. Sieber, K. Morokuma, *J. Am. Chem. Soc.* **1995**, *117*, 12366–12367.
[6] C. E. Laplaza, A. L. Odom, W. M. Davis, C. C. Cummins, J. D. Protasiewicz, *J. Am. Chem. Soc.* **1995**, *117*, 4999–5000.
[7] J.-P. F. Cherry, A. R. Johnson, L. M. Baraldo, Y.-C. Tsai, C. C. Cummins, S. V. Kryatov, E. V. Rybak-Akimova, K. B. Capps, C. D. Hoff, C. M. Haar, S. P. Nolan, *J. Am. Chem. Soc.* **2001**, *123*, 7271–7286.
[8] J. C. Peters, A. L. Odom, C. C. Cummins, *Chem. Commun.* **1997**, 1995–1996.
[9] J. B. Greco, J. C. Peters, T. A. Baker, W. M. Davis, C. C. Cummins, G. Wu, *J. Am. Chem. Soc.* **2001**, *123*, 5003–5013.
[10] J. C. Peters, L. M. Baraldo, T. A. Baker, A. R. Johnson, C. C. Cummins, *J. Organomet. Chem.* **1999**, *591*, 24–35.
[11] G. Christian, R. Stranger, S. Petrie, B. F. Yates, C. C. Cummins, *Chem. Eur. J.* **2007**, *13*, 4264–4272.
[12] K. M. Neyman, V. A. Nasluzov, J. Hahn, C. R. Landis, N. Rösch, *Organometallics* **1997**, *16*, 995–1000.
[13] G. Christian, J. Driver, R. Stranger, *Faraday Discuss.* **2003**, *124*, 331–341.
[14] G. Christian, R. Stranger, *Dalton Trans.* **2004**, 2492–2495.
[15] G. Christian, R. Stranger, B. F. Yates, *Inorg. Chem.* **2006**, *45*, 6851–6859.
[16] G. Christian, R. Stranger, B. F. Yates, D. C. Graham, *Dalton Trans.* **2005**, 962–968.
[17] J. C. Peters, J. P. F. Cherry, J. C. Thomas, L. Baraldo, D. J. Mindiola, W. M. Davis, C. C. Cummins, *J. Am. Chem. Soc.* **1999**, *121*, 10053–10067.
[18] G. te Velde, F. M. Bickelhaupt, E. J. Baerends, C. Fonseca Guerra, S. J. A. Van Gisbergen, J. G. Snijders, T. Ziegler, *J. Comput. Chem.* **2001**, *22*, 931–967.
[19] C. Fonseca Guerra, J. G. Snijders, G. Te Velde, E. J. Baerends, *Theor. Chem. Acc.* **1998**, *99*, 391–403.
[20] "Theoretical Chemistry" in *Amsterdam Density Functional (ADF)*, vol. SCM, **2002**.
[21] S. H. Vosko, L. Wilk, M. Nusair, *Can. J. Phys.* **1980**, *58*, 1200–1211.
[22] A. D. Becke, *Phys. Rev. A* **1988**, *38*, 3098–3100.
[23] J. P. Perdew, *Phys. Rev. B* **1986**, *33*, 8822–8824.
[24] G. T. Velde, E. J. Baerends, *J. Comput. Phys.* **1992**, *99*, 84–98.
[25] L. Versluis, T. Ziegler, *J. Chem. Phys.* **1988**, *88*, 322–328.
[26] E. van Lenthe, E. J. Baerends, J. G. Snijders, *J. Chem. Phys.* **1993**, *99*, 4597–4610.
[27] E. van Lenthe, E. J. Baerends, J. G. Snijders, *J. Chem. Phys.* **1994**, *101*, 9783–9792.
[28] E. van Lenthe, A. Ehlers, E. J. Baerends, *J. Chem. Phys.* **1999**, *110*, 8943–8953.
[29] L. Y. Fan, T. Ziegler, *J. Phys. Chem.* **1992**, *96*, 6937–6941.
[30] L. Y. Fan, T. Ziegler, *J. Chem. Phys.* **1992**, *96*, 9005–9012.
[31] C. C. Pye, T. Ziegler, *Theor. Chem. Acc.* **1999**, *101*, 396–408.
[32] T. K. Woo, L. Cavallo, T. Ziegler, *Theor. Chem. Acc.* **1998**, *100*, 307–313.
[33] M. Clark, R. D. Cramer, N. Vanopdenbosch, *J. Comput. Chem.* **1989**, *10*, 982–1012.
[34] A. K. Rappe, C. J. Casewit, K. S. Colwell, W. A. Goddard, W. M. Skiff, *J. Am. Chem. Soc.* **1992**, *114*, 10024–10035.

Received: March 20, 2007
Published Online: June 19, 2007

